Sequential Reduction of Mitochondrial Transmembrane Potential and Generation of Reactive Oxygen Species in Early Programmed Cell Death

By Naoufal Zamzami,* Philippe Marchetti,* Maria Castedo,* Didier Decaudin,* Antonio Macho,* Tamara Hirsch,* Santos A. Susin,* Patrice X. Petit,‡ Bernard Mignotte,‡ and Guido Kroemer*

*From the *Centre National de la Recherche Scientifique, Unité Propre de Recherche 420, F-94801 Villejuif, France; and the ‡Centre de Génétique Moléculaire, Centre National de la Recherche Scientifique, Unité Propre de Recherche 2420, F-91190 Gif sur Yvette, France*

Summary

Programmed cell death (PCD) is a physiological process commonly defined by alterations in nuclear morphology (apoptosis) and/or characteristic stepwise degradation of chromosomal DNA occurring before cytolysis. However, determined characteristics of PCD such as loss in mitochondrial reductase activity or cytolysis can be induced in enucleated cells, indicating cytoplasmic PCD control. Here we report a sequential disregulation of mitochondrial function that precedes cell shrinkage and nuclear fragmentation. A first cyclosporin A–inhibitable step of ongoing PCD is characterized by a reduction of mitochondrial transmembrane potential, as determined by specific fluorochromes (5,5',6,6'-tetrachloro-1,1',3,3'-tetraethylbenzimidazolcarbocyanine iodide; 3,3'dihexyloxacarbocyanine iodide). Cytofluorometrically purified cells with reduced mitochondrial transmembrane potential are initially incapable of oxidizing hydroethidine (HE) into ethidium. Upon short-term in vitro culture, such cells acquire the capacity of HE oxidation, thus revealing a second step of PCD marked by mitochondrial generation of reactive oxygen species (ROS). This step can be selectively inhibited by rotenone and ruthenium red yet is not affected by cyclosporin A. Finally, cells reduce their volume, a step that is delayed by radical scavengers, indicating the implication of ROS in the apoptotic process. This sequence of alterations accompanying early PCD is found in very different models of apoptosis induction: glucocorticoid-induced death of lymphocytes, activation-induced PCD of T cell hybridomas, and tumor necrosis factor–induced death of U937 cells. Transfection with the antiapoptotic protooncogene Bcl-2 simultaneously inhibits mitochondrial alterations and apoptotic cell death triggered by steroids or ceramide. In vivo injection of fluorochromes such as 5,5',6,6'-tetrachloro-1,1',3,3'-tetraethylbenzimidazolcarbocyanine iodide; 3,3'dihexyloxacarbocyanine iodide; or HE allows for the detection of cells that are programmed for death but still lack nuclear DNA fragmentation. In particular, assessment of mitochondrial ROS generation provides an accurate picture of PCD-mediated lymphocyte depletion. In conclusion, alterations of mitochondrial function constitute an important feature of early PCD.

Programmed cell death (PCD)[1] is likely to occur during the whole lifetime of higher organisms, including early embryogenesis, to affect any cell type, and to constitute the normal fate of cells (1–3). In spite of its physiological and pathological importance, at least two major problems concerning PCD remain still elusive: (*a*) an operative definition of PCD, and (*b*) an efficient system to detect PCD in vivo.

PCD is commonly defined by characteristic morpholog-

N. Zamzami and P. Marchetti contributed equally to this work.

[1] *Abbreviations used in this paper:* CHX, cycloheximide; CsA, cyclosporin A; DCFH-DA, 2'-7'-dichlorofluorescin diacetate; $\Delta\Psi_m$, mitochondrial transmembrane potential; DEX, dexamethasone; $DiOC_6(3)$, 3,3'dihexyloxacarbocyanine iodide; Eth, ethidium; HE, hydroethidine; JC-1, 5,5',6,6'-tetrachloro-1,1',3,3'-tetraethylbenzimidazolcarbocyanine iodide; mCICCP, carbonyl cyanide m-chlorophenylhydrazone; NAO, 10-N nonyl-acridine orange; PCD, programmed cell death; PI, propidium iodide; PT, permeability transition; ROS, reactive oxygen species.

J. Exp. Med. © The Rockefeller University Press • 0022-1007/95/08/0367/11 $2.00
Volume 182 August 1995 367-377

ical alterations (apoptosis) of the nucleus (heterochromatin condensation, nuclear fragmentation, and pyknosis), as well as a stepwise degradation of nuclear DNA, first into subchromosomal fragments of 50–300 kbp, then into mono- or oligonucleosomal DNA fragments (1–3). The notion that the nucleus would be a prime target of PCD is supported by a series of observations: (*a*) direct DNA damage may cause PCD; (*b*) during apoptosis, nuclear disintegration precedes cytolysis; (*c*) in numerous experimental systems, a strict correlation between modulation of PCD and nuclear apoptosis is observed; (*d*) agents that inhibit DNA-degrading enzymes retard cytolysis of cells undergoing PCD; and (*e*) a number of PCD-regulatory oncogene products function in the nucleus (3, 4). However, recent studies invalidate the concept that alterations of the nucleus are obligatory events in PCD. Although agents that inhibit endonucleases such as aurintricarboxylic acid, zinc, and calcium chelators retard cytolysis in many systems, they do not ultimately prevent cell death (for review see reference 5). More importantly, PCD can be induced in enucleated cells (cytoblasts), provided that PCD is defined by assessing nonnuclear parameters, a process in which reduction of mitochondrial activity precedes loss of membrane integrity and which is inhibited by the antiapoptotic protooncogene product Bcl-2 (6, 7). Therefore, events occurring independently or upstream of nuclear alterations have a major impact in the regulation and/or execution of PCD.

One of the cardinal features of PCD is that, early during the process of death, cells undergo changes of membrane physicochemistry allowing for their recognition and elimination by neighboring cells (8). The very efficient removal of apoptotic cells in vivo probably accounts for the difficulty of detecting signs of advanced PCD, including signs of nuclear apoptosis, in vivo. This applies particularly to tissues endowed with a high phagocytic capacity, such as peripheral lymphoid organs, yet only partially to organs such as the thymus (9). Thus, even during drastic apoptosis-inducing regimes, peripheral lymphocytes isolated ex vivo fail to exhibit morphological or biochemical alterations of the nucleus. This has been shown for in vivo injection of lymphocyte-depleting doses of glucocorticoids (10), superantigens (11), and certain cytostatic drugs (12) as well as for PCD-inducing HIV infection (13, 14).

Indirect evidence obtained recently suggests that alterations in mitochondrial physiology could be involved in PCD. First, reactive oxygen species (ROS) may participate as effector molecules in PCD (15–17). Although the source of these ROS accounting for PCD execution has not been characterized, it is known that the ubiquinone complex of the respiratory chain is a major source of superoxide radicals (18). Second, lymphocytes undergoing glucocorticoid or superantigen-induced death, as well as fibroblasts transfected with a temperature-sensitive mutant of SV40 large T cell antigen, exhibit a reduction in mitochondrial transmembrane potential ($\Delta\Psi_m$) preceding nuclear DNA degradation (19, 20). The reduction in $\Delta\Psi_m$ also concerns peripheral lymphocytes dying from PCD in vivo (19). Third, in a cell-free system, only mitochondria-enriched cytoplasma fractions are capable of inducing nuclear apoptosis (21). Fourth, members of the Bcl-2 family of apoptosis-regulatory proteins are located preferentially in the outer mitochondrial membrane (22), and, at least in one system, localization to this compartment is indispensable for apoptosis modulation (23).

Stimulated by these observations, we assessed mitochondrial function in preapoptotic cells, i.e., cells that still lack nuclear signs of PCD yet are irreversibly committed to undergoing PCD. We report here that a defined sequence of mitochondrial alterations—reduction of $\Delta\Psi_m$ followed by enhanced generation of superoxide anions— is a constant feature of early PCD. The mechanisms accounting for mitochondrial disregulation have been characterized.

Materials and Methods

Animals and In Vivo Manipulations. 6- to 10-wk-old BALB/c females received intraperitoneal injections of dexamethasone (DEX, 1 mg; Sigma Chemical Co., St. Louis, MO) or PBS as a vehicle control (200 μl) (10). In some experiments, animals received intravenous injections of nontoxic doses of the fluorochromes 5,5',6,6'-tetrachloro-1,1',3,3'-tetraethylbenzimidazolcarbocyanine iodide (JC-1; 380 μM in 200 μl PBS), 3,3'dihexyloxacarbocyanine iodide ($DiOC_6(3)$; 100 μM), and/or hydroethidine (HE; 5 mM; Molecular Probes, Inc., Eugene, OR) 20–30 min before killing.

Cells and Culture Conditions. Splenocytes were prepared on ice, depleted from erythrocytes by hypotonic lysis as described (11), and maintained in RPMI 1640 medium supplemented with 10% FCS, L-glutamine, Hepes, and antibiotics at 0–4°C until labeling and analysis. 2B4.11 T cell hybridoma cell lines stably transfected with an SFFV.neo vector containing the human *bcl-2* gene or the neomycin resistance gene only (24, 25) (kindly provided by Jonathan Ashwell, National Institutes of Health), U937 myelomonocytary cells, or WEHI-231 pre–B cells were incubated with the indicated apoptosis-inducing stimulus: 100 μM DEX; 50 μM ceramide (Sigma Chemical Co.) (26); plastic-immobilized anti-CD3 (145-2C11, coated to flat-bottomed 96-well microtiter plates [Nunc, Roskilde, Denmark] at 20 μg/ml in 100 mM Tris-HCl overnight); human rTNF-α (0.4 ng/ml; Research Diagnostics, Inc., Flanders, NJ), and/or cycloheximide (CHX, 0.5 μg/ml) (27); or anti-IgM antibodies (5 μg/ml goat anti–mouse antiserum, Southern Biotechnology Associates; Birmingham, AL) (28).

Cytofluorometry and Confocal Microscopy. For in vitro labeling, cells were exposed for 10–15 min at 37°C to JC-1 (1 μM in PBS) (29), propidium iodide (PI; 5 μg/ml), merocyanine 540 (MC540, 10 μg/ml) (30), 10-N nonyl-acridine orange (NAO; 100 nM, Molecular Probes, Inc.) (31), 2',7'-dichlorofluorescin diacetate (DCFH-DA; 5 μM) (15), $DiOC_6(3)$ (40 nM) (32), and/or HE (2 μM) (33). As a control in some experiments, cells were labeled in the presence of the uncoupling agent carbonyl cyanide m-chlorophenylhydrazone (mClCCP, 50 μM; Sigma Chemical Co.). In a further series of control experiments, cells were incubated in the presence of *tert*-butylhydroperoxide (50 mM, 2 min, RT; Sigma Chemical Co.), menadione (1 mM, 1 h, 37°C; Sigma Chemical Co.), rotenone (1 mM, 1.5 h, 37°C), or mClCCP (5 μM, 1 h, 37°C), washed twice, and labeled with NAO. Unless otherwise indicated, in all experiments involving splenocytes, forward and side scatters were gated on the major population of normal-sized lymphoid cells. The frequency of cells having lost part of their chromosomal DNA

(subdiploid cells) was determined by ethanol permeabilization and PI staining as described (34). Analyses were performed on a cytofluorometer (Epics Profile; Coulter Corp., Hialeah, FL) or on a confocal microscope (Acas 570; Meridian Instruments, Inc., Okemos, MI).

Functional Studies of Purified Cell Populations. For cytofluorometric purification, splenocytes were first depleted from cellular debris by density gradient (Ficoll Hypaque; Pharmacia LKB, Uppsala, Sweden) centrifugation and then labeled with $DiOC_6(3)$ plus HE. Lymphocytes with normal size were gated on via the forward light scatter and were sorted immediately on a cytofluorometer (Elite; Becton Dickinson and Co., San Jose, CA; 10^4 cells per second, windows as in Fig. 2) and recovered in complete medium on ice. Cells were incubated in the presence or absence of cyclosporin A (CsA) (10 μM, Sandoz Pharmaceuticals Corp., East Hanover, NJ), rotenone (1 mM), ruthenium red (100 μM), digitonin (1 μM), antimycin A (50 μM), mClCCP (50 μM), A23187 (2 μM), *N-t*-butyl-α-phenylnitrone (50 μM), trolox (230 μM), and L-ascorbate (600 μM, Sigma Chemical Co.) at doses previously determined to give optimal effects. Cells (minimum 20,000 cells per tube) were kept in media supplemented with the indicated reagents for 15 min at 4°C, followed by relabeling with $DiOC_6(3)$ plus HE and reanalysis on the cytofluorometer.

Results and Discussion

Reduced $\Delta\Psi_m$ and Enhanced ROS Generation Characterize DEX-primed Splenocytes In Vivo. Freshly isolated splenocytes from DEX-primed mice exhibit intact DNA, even when recovered during the phase of maximum reduction of splenic cellularity (12 h after injection of 1 mg DEX) (10, 19). Although these cells lack established signs of nuclear PCD, they exhibit a diminution of $\Delta\Psi_m$, as quantitated by means of the fluorochrome JC-1 (Fig. 1, *A* and *B*). JC-1 incorporates into mitochondria, where it either forms monomers (fluorescence in green, 527 nm) or, at high transmembrane potentials, aggregates (fluorescence in red, 590 nm) (29). As compared with control cells, DEX-primed splenocytes exhibit a reduced JC-1 aggregation, a finding that indicates a drop in $\Delta\Psi_m$. Such a staining pattern is obtained when splenocytes are incubated in vitro (15 min, 37°C) in the presence of JC-1. Very similar results are seen when JC-1 labeling is performed in vivo by injecting a nontoxic dose of the fluorochrome into the animal, followed by a phase of in vivo incubation (30 min) and ex vivo fluorescence analysis of freshly isolated cells (Fig. 1 *A*). This demonstrates that $\Delta\Psi_m$ reduction actually does occur in vivo. Interestingly, DEX-primed cells with low $\Delta\Psi_m$ display a synchronous reduction of JC-1 aggregation in all mitochondria-containing cytoplasma areas (Fig. 1 *B*). Uncoupling of DEX-primed cells with mClCCP can further reduce JC-1 incorporation into cells by 0.3–0.5 logs (Fig. 1 *A*), indicating that the $\Delta\Psi_m$ is not completely disrupted.

In a further series of experiments, JC-1 was replaced by another fluorochrome, $DiOC_6(3)$, which incorporates into mitochondria in strict nonlinear dependence of $\Delta\Psi_m$ and emits exclusively within the spectrum of green light (32). As reported (19), staining with $DiOC_6(3)$ revealed the presence of a major subpopulation of $\Delta\Psi_m^{low}$ cells within the spleen of DEX-primed animals (see Figs. 1 *C* and 3 *A*). Cells were labeled simultaneously with HE, a substance that is oxidized by ROS to become ethidium (Eth) and to emit red fluorescence (33). Splenocytes from DEX-primed animals contain two distinct $DiOC_6(3)^{low}$ ($\Delta\Psi_m^{low}$) subpopulations, one that exhibits low ROS formation (HE^- cells), comparable to that of $\Delta\Psi_m^{high}$ cells, and another one that is characterized by an enhanced HE → Eth conversion (HE^+ cells). The $DiOC_6(3)$/HE staining patterns obtained in vivo (see Fig. 1 *C*) and in vitro (see Figs. 2 and 3 *A*) are comparable, indicating again that $\Delta\Psi_m$ diminution and enhanced HE oxidation are not in vitro artifacts and actually occur in vivo. Since DEX-primed splenocytes do not stain with 2',7'-dichlorofluorescin diacetate (which measures H_2O_2 formation [15, 33, 35]) (Fig. 2) yet become capable of converting HE into Eth (which is especially sensitive to superoxide anions [33, 35]), it appears that the ROS responsible for HE conversion is superoxide anion.

Minor populations of $\Delta\Psi_m^{low}$ or HE^+ cells were also found in spleens from unprimed animals (Fig. 1), a fact that can be attributed either to cell damage occurring during splenocyte purification or to spontaneous cell death, which is relatively frequent in the spleen (36, 37). Nonetheless, the frequency of such cells is strongly increased in DEX-treated animals.

Sequential $\Delta\Psi_m$ Reduction and ROS Generation in Preapoptotic Cells. It may be assumed that $DiOC_6(3)$/HE staining of DEX-primed splenocytes provides a snapshot of different stages of ongoing preapoptosis. To determine the exact precursor–product relationship of these stages, the populations defined by simultaneous labeling with $DiOC_6(3)$ and HE were purified by cytofluorometric sorting while gating on normal-sized cells in the forward light scatter (Fig. 3 *A*). Transmission electron microscopy revealed no major alterations in nuclear morphology in any of these fractions (not shown). Upon relabeling and reanalysis, purified cells cultured in vitro for 1 h at 37°C, but not controls kept at 4°C, exhibit characteristic phenotypic alterations. A minor population of $\Delta\Psi_m^{high}HE^-$ cells becomes $\Delta\Psi_m^{low}HE^-$. A fraction of $\Delta\Psi_m^{low}HE^-$ cells acquires a $\Delta\Psi_m^{low}HE^+$ phenotype. $\Delta\Psi_m^{low}HE^+$ splenocytes conserve their phenotype with the exception of size; forward scatter analysis reveals that a high percentage of these cells collapses during short-term in vitro culture (Fig. 3 *A*) and thus exhibits a characteristic of incipient apoptosis (38). None of the purified populations contains a significant percentage (<2%) of subdiploid cells, as assessed by analysis of the DNA content. In vitro culture, followed by assessment of DNA content, reveals that $\Delta\Psi_m^{low}HE^+$ cells are the first to undergo nuclear fragmentation, whereas their HE^- precursors are comparatively resistant to nuclear DNA loss (Fig. 3 *B*). These results provide evidence that DEX-primed splenocytes first reduce their $\Delta\Psi_m$ and then hyperproduce ROS, reduce in size, and finally undergo endonucleolysis. Kinetic analysis of DEX-induced splenocyte death corroborates this scenario (Fig. 3 *C*), which is not restricted to one particular PCD induction system (see below). It appears that labeling with HE provides a more accurate picture of ongoing cell depletion than assessment of $\Delta\Psi_m$ by

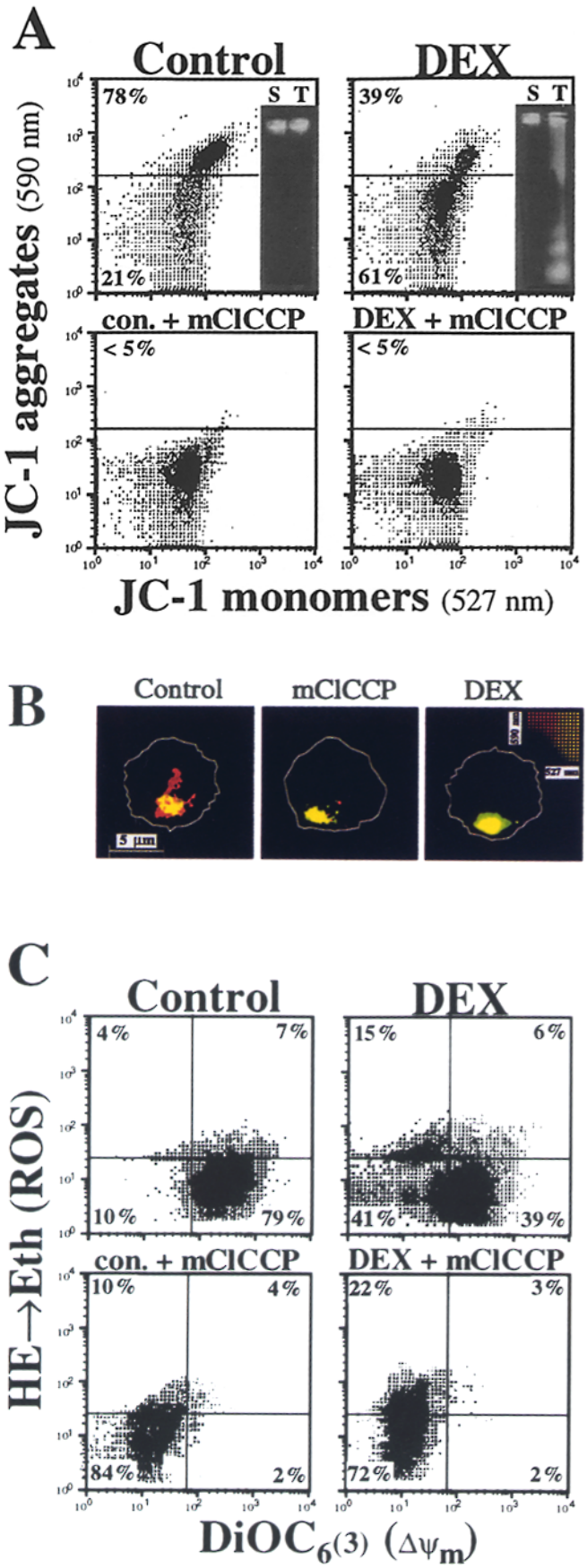

$DiOC_6(3)$ or JC-1. Whereas a significant reduction of $\Delta\Psi_m$ precedes the DEX-driven loss in splenic cellularity, enhanced HE staining is observed only when the number of splenic cells is actually diminishing (Fig. 3 *C*).

Different Mechanisms Are Involved in $\Delta\Psi_m$ Reduction and Mitochondrial ROS Generation. The notion that the $\Delta\Psi_m{}^{low}HE^-$ and $\Delta\Psi_m{}^{low}HE^+$ phenotypes constitute discrete stages of preapoptosis is underscored by manipulations selectively affecting either the loss in $\Delta\Psi_m$ or the production of ROS (Fig. 4). FACS®-purified cells were cultured 1 h in the presence of different substances known to affect mitochondrial function, followed by relabeling with $DiOC_6(3)$/HE and reanalysis. In the model of DEX-induced splenocyte apoptosis, the transition from the $\Delta\Psi_m{}^{high}HE^-$ to the $\Delta\Psi_m{}^{low}HE^-$ state, which normally ensues in in vitro culture at 37°C (Fig. 3 *A*), is prevented by CsA. Thus, CsA, an agent previously shown to inhibit the opening of mitochondrial inner membrane megachannels in isolated mitochondria (39) and in anoxia-damaged hepatocytes or myocardial cells (40, 41), also inhibits PCD-associated $\Delta\Psi_m$ loss in lymphocytes. This may indicate that, during the initial phase of PCD, $\Delta\Psi_m$ reduction involves a mitochondrial permeability transition (PT) mediated by mitochondrial inner membrane megachannels.

Although CsA inhibits $\Delta\Psi_m{}^{low}$ reduction, it does not affect the transition from the $\Delta\Psi_m{}^{low}HE^-$ to the $\Delta\Psi_m{}^{low}HE^+$ stage. ROS production by $\Delta\Psi_m{}^{low}$ cells is selectively blocked by inhibition of mitochondrial electron transport in complex I by rotenone as well as by the hexavalent cation ruthenium red, a specific inhibitor of the mitochondrial calcium uniport (42, 43). To allow for optimal diffusion of ruthenium red to its site of action, the inner mitochondrial membrane, cells must be partially permeabilized with digitonin (44). Digitonin does not cause a reduction in $\Delta\Psi_m$ per se, since it only permeabilizes cholesterol-containing membranes (45) and the inner mitochondrial membrane is essentially cholesterol free

Figure 1. Assessment of $\Delta\Psi_m$ in splenic T cells from DEX-primed animals. (*A*) In vivo assessment of DEX-induced shift in $\Delta\Psi_m$. 12 h after intraperitoneal administration of DEX or PBS as vehicle control, animals were injected intravenously with JC-1. After 30 min of in vivo incubation, splenocytes were recovered and subjected to cytofluorometry while gating on normal sized lymphocytes. As a control, cells were incubated before analysis with mClCCP (50 µM; 15 min, 37°C), an uncoupling agent that completely abolishes the $\Delta\Psi_m$. In addition, DNA from 2×10^6 splenocytes (*S*) from PBS- or DEX-primed animals was subjected to gel electrophoresis as described (11), not revealing any DNA degradation among DEX-primed splenocytes (*insets*). Thymocytes (*T*), which, in contrast to peripheral lymphocytes, do undergo massive DNA fragmentation in vivo (9) in response to DEX, were included as positive controls. Results are representative of three independent experiments. (*B*) Confocal microscopy of splenocytes labeled ex vivo. Splenic T cells from animals injected with PBS or DEX as above were stained in vitro with the fluorescence dye JC-1 (1 µM, 15 min, 37°C). As a control, cells were labeled with JC-1 in the presence of mClCCP (5 µM; 15 min, 37°C). (*C*) Simultaneous in vivo detection of $\Delta\Psi_m$ and ROS production. After intraperitoneal application of DEX or PBS (12 h before analysis), animals were injected intravenously with $DiOC_6(3)$ and HE (20 min before analysis), respectively, followed by cytofluorometric analysis. Mitochondria were uncoupled with the protonophore mClCCP, as in *B*.

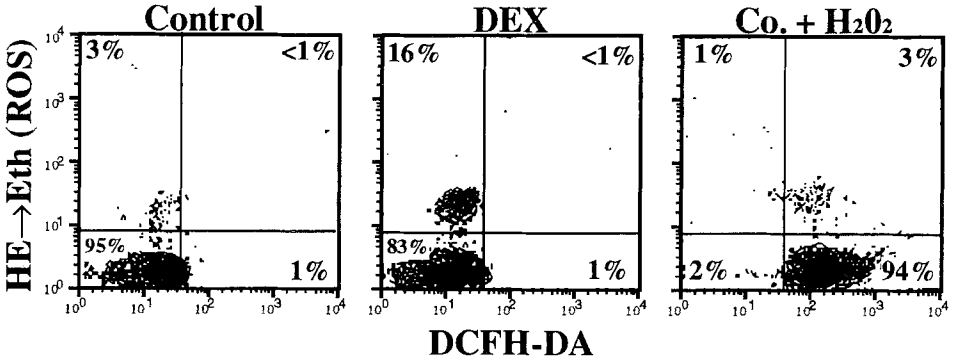

Figure 2. Simultaneous assessment of ROS generation by HE and DCFH-DA. Splenocytes from control and DEX-primed animals (1 mg i.p., 12 h before analysis) were labeled in vitro with HE (2 μM) and DCFH-DA (5 μM) for 10 min at 37°C, followed by cytofluorometric analysis. As a positive control for DCFH-DA labeling, cells from PBS-treated mice were incubated for 2 min in the presence of 15 mM H_2O_2 and washed twice before labeling.

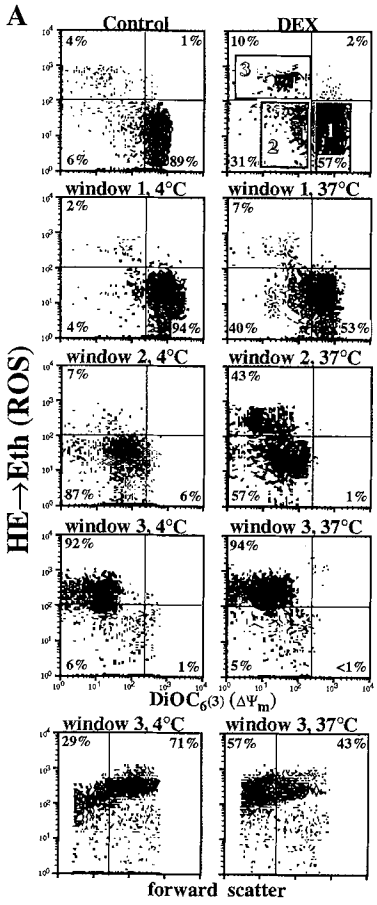

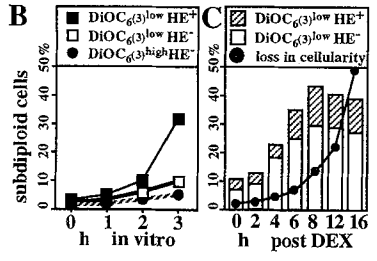

Figure 3. Relationship between $\Delta\Psi_m$ reduction and ROS generation. (*A*) Determination of the precursor product relationship of FACS®-purified populations. Splenocytes from DEX-primed BALB/c mice (1 mg i.p., 12 h before analysis) or vehicle controls were kept on ice and incubated with a mixture of $DiOC_6(3)$ (40 nM in PBS) and HE (2 μM) for 10 min at 37°C immediately before cytofluorometric analysis. Purified cells from windows 1–3 were kept for 60 min at 4°C or 37°C, followed by relabeling and reanalysis under identical conditions. Among cells from windows 1 and 2, no significant (<10%) reduction in cell size was observed during 1 h of culture at 37°C (not shown). Accordingly, gating on normal-sized cells was maintained during reanalysis of these populations. In contrast, upon reanalysis of fraction 3, a high portion of cells displayed a temperature-dependent reduction in size (*lower panel*). Results are typical for six independent experiments. (*B*) Loss of nuclear DNA of different cell fractions. Cells purified as in *A* were cultured during the indicated interval, followed by determination of the frequency of subdiploid cells. (*C*) Kinetics of the loss in $\Delta\Psi_m$ and ROS production from DEX-primed splenocytes. Mice received DEX injections (1 mg i.p.). After the indicated interval, splenocytes were recovered and labeled ex vivo as in *A*. DNA hypoploidy concerns <1% of cells for any time point. Moreover, the reduction in viable splenocytes recovered (mean values of three animals) is computed.

(46). Complete uncoupling of mitochondria by addition of the protonophore mClCCP accelerates ROS production. Similarly, the calcium ionophore A23187 accelerates the transition from the $\Delta\Psi_m^{low}HE^-$ to the $\Delta\Psi_m^{low}HE^+$ stage. Therefore, ROS responsible for HE → Eth conversion are produced by mitochondria in a calcium-dependent fashion. Accordingly, control substances that affect nonmitochondrial pathways of ROS generation fail to affect the transition from the $DiOC_6(3)^{low}HE^-$ to the $DiOC_6(3)^{low}HE^+$ stage. This applies to inhibitors of lipoxygenase (10 μM nordihydroguaiaretic acid), cycloxygenase (500 μM indomethacin), monoamine oxidase (1.5 mM pargyline), xanthine oxidase (300 μM allopurinol), nitric oxide synthetase (100 μM N^G-methyl-L-arginine), pyrrolidinedithiocarbamate (100 μM), which stops the Fenton reaction converting H_2O_2 into superoxide anions, and diphenylene iodonium (0.1 μM), an inhibitor of NADPH oxidase and other flavin oxidases (47) (not shown). In contrast, antimycin A, an agent that leads to increased superoxide anion generation at sites proximal to the complex III of electron transport (48), enhances the $\Delta\Psi_m^{low}HE^-/\Delta\Psi_m^{low}HE^+$ transition (Fig. 4). This underscores that electron transport is still going on in $\Delta\Psi_m^{low}$ cells.

At a final level, the shrinkage of $\Delta\Psi_m^{low}HE^+$ cells is selectively inhibited by substances that suppress mitochondrial ROS generation (rotenone, ruthenium red), as well as by antioxidants such as the vitamin E derivative trolox, alone or in

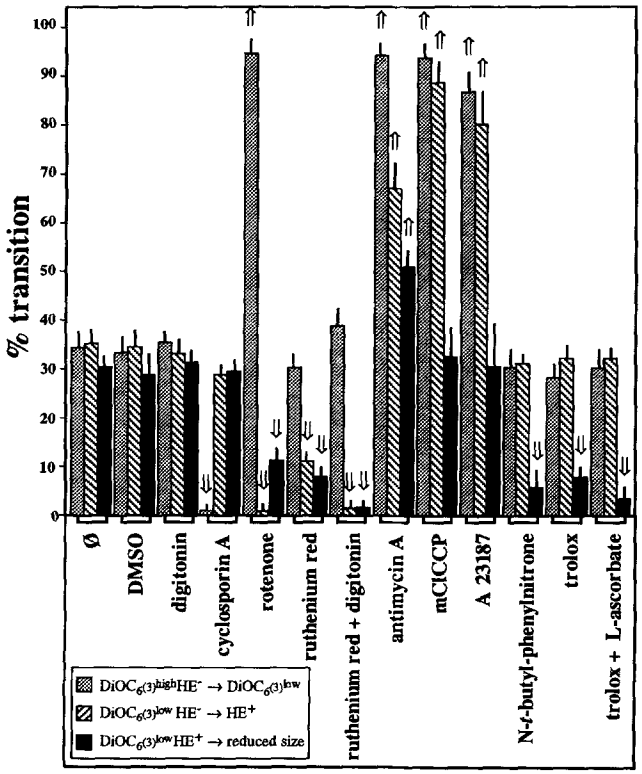

Figure 4. Modulation of progressing preapoptosis reveals independent mechanisms of $\Delta\Psi_m$ reduction and ROS generation. DEX-primed splenocytes were sorted cytofluorometrically into three normal-sized populations: $DiOC_6(3)^{high}HE^-$, $DiOC_6(3)^{low}HE^-$, and $DiOC_6(3)^{low}HE^+$ cells, followed by in vitro culture (1 h, 37°C), relabeling, and reanalysis (manipulation similar as in Fig. 3 *A*). The transition to the immediately posterior stage of preapoptosis is indicated for each subpopulation in different conditions of in vitro culture. Background values obtained in control cultures kept at 4°C (Fig. 3 *A*) were subtracted from experimental values. Results (±SEM) are pooled from five different experiments. Each agent was evaluated at least three times. Ruthenium red was diluted in DMSO (final concentration of 1%). Arrows indicate a significant ($P < 0.01$, Student's *t* test) increase or decrease of transition processes as compared with controls.

combination with L-ascorbate, or the radical scavenger *N-t*-butyl-α-phenylnitrone (Fig. 4). This observation confirms that ROS are PCD effector molecules.

In synthesis, these data indicate that $\Delta\Psi_m$ reduction and enhanced mitochondrial ROS generation indeed represent two clearly distinct phases of the preapoptotic process. Only after $\Delta\Psi_m$ has dropped are ROS generated and do they participate in the perturbation of mitochondrial membranes (see below), as well as in later manifestations of PCD such as cell shrinkage.

Enhanced ROS Generation Is Accompanied by Local Membrane Perturbation but Precedes Alterations of the Cell Membrane. To determine whether ROS generated in mitochondria have a direct local impact on mitochondrial membranes, the amount of intact cardiolipin, a molecule restricted to the inner mitochondrial membrane (46, 49), was determined by means of the fluorochrome NAO. NAO interacts stoichiometrically with intact cardiolipin (1:2) (31), and this interaction is not influenced by the mitochondrial energy state (50). As shown in Fig. 5 *A*, only two major populations can be detected in the spleen, one characterized by low HE → Eth conversion and normal NAO staining (NAO^{high} cells) and a second one marked by enhanced HE oxidation and reduced NAO staining. The frequency of HE^+NAO^{low} cells increases in DEX-primed spleens. Control experiments (Fig. 5 *B*) demonstrate that the reduction of $\Delta\Psi_m$ by incubation with rotenone does not affect the labeling with NAO. In contrast, incubation of cells with an exogenous source of ROS (*tert*-butylhydroperoxide) or inducers of ROS generation (menadione or mClCCP) causes a reduction in NAO staining. This reduction is immediate after a short incubation with *tert*-butylhydroperoxide (2 min, Fig. 5 *B*) or an equivalent concentration of H_2O_2 (2 min, not shown), suggesting that it could result from direct cardiolipin oxidation. Thus, the ROS responsible for HE → Eth conversion may be suspected of causing an immediate oxidation of mitochondrial compounds. Moreover, the fact that most if not all HE^- cells exhibit a normal NAO^{high} phenotype (Fig. 5 *A*) indicates that $\Delta\Psi_m{}^{low}HE^-$ cells still possess normal inner mitochondrial membranes.

As shown above, DEX-primed splenocytes of normal size contain a significant number of HE^+ cells (Figs. 1 *C*, 2, 3 *A*, and 5 *C*), which undergo cell shrinkage upon in vitro culture (Fig. 3 *B*). In contrast, only comparatively small cells exhibit alterations of the cell membrane that have been reported to accompany PCD: an enhanced cell permeability, as indicated by incorporation of PI (51), and increased labeling with MC540 (30, 52) (Fig. 5 *C*). MC540 is thought to measure apoptosis-associated alterations in lipid packaging (30), such as aberrant exposure of phosphatidylserine residues on the outer leaflet of the membrane (53) mediating the phagocyte-mediated recognition and removal of apoptotic cells. The fraction of small $PI^{intermediate/high}$ $MC540^+$ splenocytes was increased in DEX-primed animals (Fig. 5 *C*).

In synthesis, this set of data suggests that ROS generation causes an immediate damage of the inner mitochondrial membrane, yet it precedes cells shrinkage and associated plasma membrane alterations.

Correlation between Mitochondrial Perturbation and Apoptosis Induction in Different In Vitro Models of PCD. Reduction in $\Delta\Psi_m$ and subsequent ROS hyperproduction are observed in several in vitro models of physiological PCD, i.e., models in which nontoxic agents were used to induce PCD in susceptible target cells: TNF-α in U937 cells and anti-IgM in WEHI 231 pre-B cells, as well as CD3 cross-linking in T cell hybridomas (Fig. 6). Ceramide, a second messenger involved in the mediation of some PCD types (26, 54), also causes these effects. In all of these systems, alterations in mitochondrial function precede DNA fragmentation and nuclear DNA loss. Thus, it appears that mitochondrial derangement is a constant feature of PCD occurring independently of the PCD-inducing stimulus.

In T cell hybridomas, transfection-enforced hyperexpression of the antiapoptotic protooncogene *bcl-2* retards $\Delta\Psi_m$ diminution and ROS generation, as well as subsequent nuclear hypoploidy in response to DEX and ceramide. This finding is in agreement with previous data suggesting a Bcl-

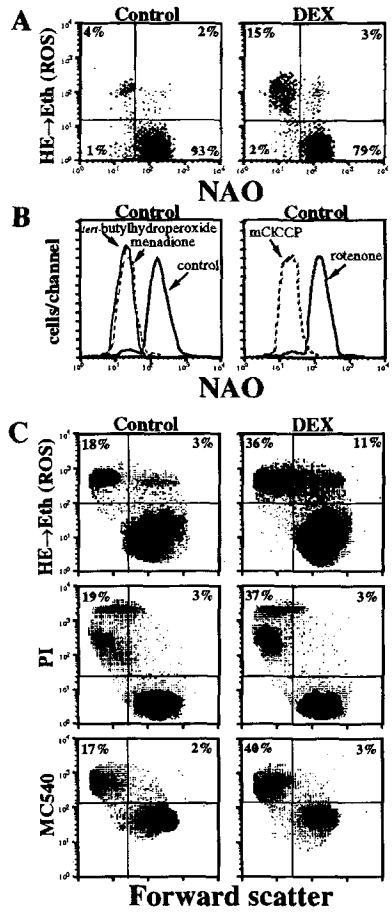

Figure 5. Increased mitochondrial ROS generation is accompanied by reduced staining with NAO, yet it precedes apoptosis-associated alterations of the plasma membrane. (*A*) Simultaneous detection of ROS generation and cardiolipin. Cells from DEX-primed mice (1 mg, 12 h before analysis) or controls were stained simultaneously with HE and NAO as described in Materials and Methods, followed by cytofluorometric analysis. NAO fluorescence was exclusively determined in FL1, and, after appropriate compensation, HE fluorescence was determined in FL3. (*B*) Effects of ROS generation of NAO staining. Control splenocytes were incubated in the presence of *tert*-butylhydroperoxide (5 mM, 2 min, RT), menadione (1 mM, 1 h, 37°C), mClCCP (50 μM, 1 h, 37°C), or rotenone (1 mM, 1.5 h, 37°C), washed, and stained with NAO. Parallel stainings with HE and $DiOC_6(3)$ revealed that rotenone-treated cells had a $DiOC_6(3)^{low}HE^-$, whereas menadione gave rise to a $DiOC_6(3)^{low}HE^+$ phenotype (not shown). (*C*) Correlation between cell size and PCD-associated changes. Cells from control and DEX-treated animals were labeled with HE, PI, or MC540. The cell size determined by means of the forward scatter (linear scale) was plotted against fluorescence (logarithmic scale). Data are representative of three different experiments.

2-mediated reduction of ROS production (16) and/or ROS action (15) during apoptosis. In contrast, Bcl-2, which is comparatively inefficient in preventing antigen receptor-induced PCD (24, 25, 28), does not affect the anti-CD3-triggered $\Delta\Psi_m$ reduction, ROS production, and loss in nuclear DNA of T cell hybridomas (Fig. 6). This underscores the strict correlation between PCD and mitochondrial alterations. Moreover, these data suggest that $\Delta\Psi_m$ reduction and subsequent ROS generation are involved both in Bcl-2-inhibited and in Bcl-2-resistant pathways of PCD.

Concluding Remarks. In this paper, we decipher a sequence of discrete steps of preapoptosis, i.e., of PCD stages occurring before the nucleus or nuclear DNA are fragmented (Fig. 7). The first alteration that distinguishes cells induced to undergo PCD from normal cells is a fall in $\Delta\Psi_m$, detectable by reduced labeling with $DiOC_6(3)$ or diminished JC-1 aggregation. Thereafter, uncoupled mitochondria hyperproduce superoxide anion (detectable by enhanced HE → Eth conversion) and simultaneously exhibit a perturbation of the inner mitochondrial membrane (detectable as reduced labeling with NAO). At this stage, cells still possess a normal size, normal dye exclusion capacity (measured by labeling with PI), and normal cell membrane characteristics (assessed by MC540). These parameters are only affected in a subsequent step of preapoptosis, the last detectable in vivo, which involves near simultaneous cell shrinkage, increase in membrane permeability, and alteration of lipid packaging, yet still intact DNA.

When integrated with the data available in the literature, the results reported in this paper strongly suggest that reduction of $\Delta\Psi_m$, concomitant with uncoupling of mitochondrial electron transport and ATP synthesis (20, 55), causes increased generation of ROS, which, in turn, are important mediators of apoptosis (15–17). In accord with this hypoth-

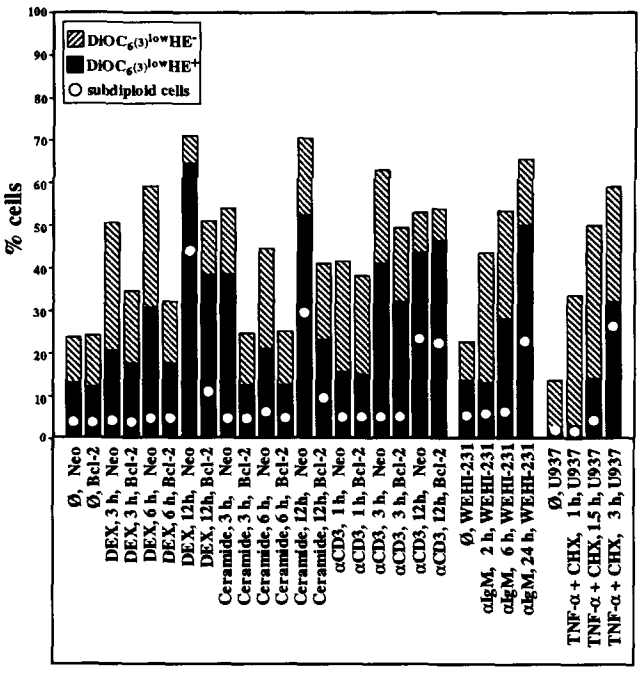

Figure 6. Correlation between $\Delta\Psi_m$ reduction, ROS generation, and nuclear apoptosis in different systems. 2B4.11 T cell hybridoma cell lines stably transfected with human *bcl-2* gene or the vector only (Neo), U937 myelomonocytary cells, or WEHI-231 pre-B cells were incubated with the indicated apoptosis-inducing stimulus: 100 μM DEX; 50 μM ceramide; immobilized anti-CD3; TNF-α (0.4 ng/ml) plus CHX (0.5 μg/ml); or anti-IgM antibodies (5 μg/ml goat anti-mouse antiserum). After the indicated interval, the frequency of $DiOC_6(3)^{high}HE^-$, $DiOC_6(3)^{low}HE^-$ and $DiOC_6(3)^{low}HE^+$ was assessed. Loss in nuclear DNA content was measured by PI staining of ethanol-permeabilized cells.

esis, direct inhibition of mitochondrial DNA replication, blockade of the respiratory chain, and induction of mitochondrial ROS generation cause PCD in lymphocytes and neurons (15, 37, 56, 57). Moreover, blockade of mitochondrial protein synthesis with doxycycline as well as inhibition of mitochondrial electron transport with low doses of rotenone renders glucocorticoid-resistant cell lines sensitive to PCD induction by DEX (55, 58). The $\Delta\Psi_m$ reduction, which we observe as a constant feature of early PCD, is per se sufficient to impair mitochondrial ATP generation, as well as mitochondrial DNA and protein synthesis (59). Accordingly, thymocyte PCD is accompanied by a strong inhibition of ATP synthesis (60), as well as by a transcription blockade selectively affecting the entire mitochondrial genome (61). Taken together, these findings argue in favor of a scenario in which breakdown of mitochondrial function, perturbation of intermediate metabolism, and/or ROS generation are involved in extranuclear PCD control. Each of the phenomena reported in this paper, loss of mitochondrial function and ROS generation, would suffice to entail cell death, thus conveying a pleiotropic effector phase to PCD execution.

It has been shown previously that a human fibroblast cell line selected in EthBr to lose mitochondrial DNA (ρ^o cells) could be induced to die from apoptosis in response to staurosporine or growth factor withdrawal (62). ρ^o cells compensate for a respiratory defect via enhanced anaerobic glycolysis and thus rely on the provision of excess glucose or pyruvate. The action of the ADP/ATP translocator to import ATP into mitochondria and/or to succinate dehydrogenase allows for the maintenance of a $\Delta\Psi_m$ that is indistinguishable from that of ρ^+ controls (63), suggesting that, even in ρ^o cells, a normal $\Delta\Psi_m$ is indispensable for cell survival. L929 cells lacking mitochondrial DNA (ρ^o cells) have been reported to be relatively resistant to the cytotoxic effect of TNF, and this resistance has been attributed to a reduced generation of ROS species (64). In contrast, ρ^o L929 cells die when exposed to a combination of TNF and CHX (64). In accord with these data, we observed that ρ^o U937 cells undergo apoptosis after stimulation with TNF and CHX, although with a certain delay as compared with normal ρ^+ controls. Interestingly, ρ^o U937 cells behave exactly as ρ^+ controls in the sense that they manifest an early $\Delta\Psi_m$ loss during the TNF/CHX-driven apoptotic process that precedes DNA fragmentation. In addition, such cells hyperproduce ROS, but at a reduced rate as compared with ρ^+ cells (Marchetti, P., N. Zamzami, M. Castedo, T. Hirsch, and G. Kroemer, manuscript in preparation), in contrast to normal cells (Fig. 4). This may indicate that the mere loss of mitochondrial function as manifested by a $\Delta\Psi_m$ loss, even when mitochondrial ROS generation is abolished or reduced, can participate in the induction of apoptosis. In accord with this speculation, it has been shown that certain types of PCD, e.g., APO-1/Fas–induced apoptosis, do not require mitochondrial ROS generation (65).

As to the mechanism of apoptosis-associated mitochondrial disregulation, it is tempting to speculate that PT, a phenomenon that has been studied for decades in isolated mitochondria, might be involved in the early step of mitochondrial disregulation (66). In numerous systems, PT is partially inhibited by CsA via a mechanism involving a mitochondrial cyclophilin but not calcineurin (39–41, 66, 67). Similarly, CsA retards the initial phase of mitochondrial disregulation accompanying apoptosis of DEX-primed splenocytes (Fig. 4) and TNF-treated U937 cells (not shown). PT involves opening of mitochondrial megachannels (also termed PT pores) localized in the inner membrane, a concomitant increase in permeability to solutes with molecular masses $\leq$1,500 daltons, uncoupling with collapse of $\Delta\Psi_m$, and cessation of ATP synthesis. Interestingly, PT transition has self-amplificatory properties, in the sense that loss of matrix Ca^{2+} and glutathione, depolarization of the inner membrane, and increased oxidation of thiols, which result from megachannel opening, themselves increase the megachannel gating potential (39, 42). This explains how PT can spread in a wavelike fashion through populations of isolated mitochondria (66). Opening of the PT pores might mark a point of no return during the effector phase of ongoing PCD and could account for the apparent synchronization of $\Delta\Psi_m$ loss, which affects all mitochondria within a cell simultaneously. Synchronization of $\Delta\Psi_m$ loss between mitochondria has been observed in lymphocytic PCD (Fig. 1 *B*) as well in relatively large cells, such as sympathetic neurons undergoing apoptosis after withdrawal of nerve cell growth factor from cultures (Zamzami, N., and P. Marchetti, unpublished observation). Although CsA is an effective inhibitor of $\Delta\Psi_m$ loss in short-term experiments (Fig. 4), CsA fails to maintain mitochondrial functions and thus does not prevent DEX-induced PCD during longer incubation periods (68). In consequence, additional CsA-resistant mechanisms could participate in apoptotic PT, as has been reported for anoxia-induced hepatocyte injury (41). Shortly after the $\Delta\Psi_m$ drop, within a few hours (Fig. 3), superoxide anion radicals are generated by an uncoupled respiratory chain via a process that requires ruthenium red–sensitive calcium cycling (Fig. 4). Overproduced ROS might irreversibly inactivate mitochondrial

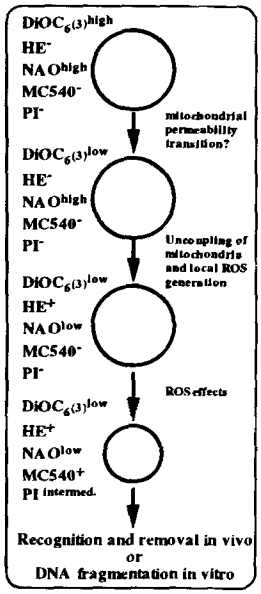

Figure 7. Phenotypes and precursor–product relationship of different stages of preapoptosis. The diagram summarizes the data obtained on in vivo DEX-primed splenocytes (Figs. 3–5). Moreover, it is confirmed in various in vitro systems of apoptosis induction (Fig. 6).

electron transport chain components and ATPase (69). This may explain why HE^+ cells have an even lower $\Delta\Psi_m$ than purified $HE^-\Delta\Psi_m^{high}$ cells (Fig. 3). Moreover, ROS produced by mitochondria accelerate cellular shrinkage, one of the first alterations accompanying apoptosis (38), as indicated by experiments involving radical scavengers (Fig. 4).

Although PT might be the consequence of multiple different pathways reported to participate in PCD regulation, including an elevation of cytosolic calcium levels (70), oxidation of cellular thiols (67), or depletion of intracellular glucose stores (71), the exact molecular mechanisms responsible for apoptotic PT remain elusive. Nonetheless, the present data provide clear evidence that alterations of mitochondrial physiology are a constant feature of very different systems of PCD induction, mark a phase of irreversible commitment to death, precede nuclear apoptosis, and allow for the in vivo detection of ongoing PCD. ROS generated from a partially uncoupled respiratory chain actively participate in the effector phase of PCD, and it is possible that mitochondria form part of the cytoplasmic PCD control instance that has been postulated by several groups (6, 21). These notions strongly suggest that an addendum should be joined to the current definition of apoptosis: Physiological PCD is a process involving an active shutdown of mitochondrial function.

We thank Maurice Geuskens (Université Libre de Bruxelles) for performing electron microscopy, as well as Benjamin Masse (Centre National de la Recherche Scientifique, Unité Propre de Recherche 420), Sophie Lafosse, and Mischal Zohar (Centre National de la Recherche Scientifique, Unité propre de Service 47) for technical assistance.

This work was supported by Association pour la Recherche sur le Cancer, Centre National de la Recherche Scientifique, Fondation pour la Recherche Médicale, Institut National de la Santé et de la Recherche Médicale, North Atlantic Treaty Organization, Leo Research Foundation, Picasso program, and Sidaction (G. Kroemer). N. Zamzami received a fellowship from Roussel Uclaf.

Address correspondence to Dr. Guido Kroemer, Centre National de la Recherche Scientifique, Unité Propre de Recherche 420, 19 rue Guy Môquet, B.P. 8, F-94801 Villejuif, France.

Received for publication 19 January 1995 and in revised form 22 March 1995.

References

1. Kerr, J.F.R., A.H. Wyllie, and A.R. Currie. 1972. Apoptosis: a basic biological phenomenon with wide-ranging implications in tissue kinetics. *Br. J. Cancer.* 26:239–257.
2. Willie, A.H. 1980. Glucocorticoid-induced thymocyte apoptosis is associated with endogenous endonuclease activation. *Nature (Lond.).* 284:555–556.
3. Cohen, J.J. 1993. Apoptosis. *Immunol. Today.* 14:126–130.
4. McConkey, D.J., P. Nicotera, and S. Orrenius. 1994. Signalling and chromatin fragmentation in thymocyte apoptosis. *Immunol. Rev.* 142:343–363.
5. Kroemer, G., and C. Martínez-A. 1994. Pharmacological inhibition of programmed lymphocyte cell death. *Immunol. Today.* 15:235-242.
6. Jacobson, M.D., J.F. Burne, and M.C. Raff. 1994. Programmed cell death and Bcl-2 protection in the absence of a nucleus. *EMBO (Eur. Mol. Biol. Organ.) J.* 13:1899–1910.
7. Schulze-Osthoff, K., H. Walczak, W. Droge, and P.H. Krammer. 1994. Cell nucleus and DNA fragmentation are not required for apoptosis. *J. Cell Biol.* 127:15–20.
8. Savill, J., V. Fadok, P. Henson, and C. Haslett. 1993. Phagocyte recognition of cells undergoing apoptosis. *Immunol. Today.* 14:131–136.
9. Surh, C.D., and J. Sprent. 1994. T-cell apoptosis detected in situ during positive and negative selection in the thymus. *Nature (Lond.).* 372:100–103.
10. Gonzalo, J.A., A. González-García, C. Martínez-A., and G. Kroemer. 1993. Glucocorticoid-mediated control of the clonal deletion and activation of peripheral T cells in vivo. *J. Exp. Med.* 177:1239–1246.
11. Kawabe, Y., and A. Ochi. 1991. Programmed cell death and extrathymic reduction of $V\beta8^+$ $CD4^+$ T cells in mice tolerant to *Staphylococcus aureus* enterotoxin B. *Nature (Lond.).* 349: 245–248.
12. Matsubara, K., M. Kubota, K. Kuwakado, H. Hirota, Y. Wakazono, Y. Akiyama, H. Mikawa, and S. Adachi. 1994. Induction of apoptosis in childhood acute leukemia by chemotherapeutic agents: failure to detect evidence of apoptosis in vivo. *Eur. J. Haematol.* 52:47–52.
13. Groux, H., G. Torpier, D. Monté, Y. Mouton, A. Capron, and J.C. Ameisen. 1992. Activation-induced death by apoptosis in $CD4^+$ T cells from human immunodeficiency virus–infected asymptomatic individuals. *J. Exp. Med.* 175: 331–340.
14. Meyaard, L., S.A. Otto, R.R. Jonker, M.J. Mijnster, R.P.M. Keet, and F. Miedema. 1992. Programmed cell death in HIV-1 infection. *Science (Wash. DC).* 257:217–219.
15. Hockenbery, D.M., Z.N. Oltvai, X.-M. Yin, C.L. Milliman, and S.J. Korsmeyer. 1993. Bcl-2 functions in an antioxidant pathway to prevent apoptosis. *Cell.* 75:241–251.
16. Kane, D.J., T.A. Sarafian, R. Anton, H. Hahn, E.B. Gralla, J.S. Valentine, T. Örd, and D.E. Bredesen. 1993. Bcl-2 inhibition of neural death: decreased generation of reactive oxygen

species. *Science (Wash. DC).* 262:1274–1277.
17. Sandstrom, P.A., M.D. Mannie, and T.M. Buttke. 1994. Inhibition of activation-induced death in a T cell hybridoma by thiol antioxidants: oxidative stress as a mediator of apoptosis. *J. Leukocyte Biol.* 55:221–226.
18. Richter, C. 1993. Pro-oxidants and mitochondrial Ca^{2+}: their relationship to apoptosis and oncogenesis. *FEBS Lett.* 325: 104–107.
19. Zamzami, N., P. Marchetti, M. Castedo, C. Zanin, J.-L. Vayssière, P.X. Petit, and G. Kroemer. 1995. Reduction in mitochondrial potential constitutes an early irreversible step of programmed lymphocyte death in vivo. *J. Exp. Med.* 181:1661–1672.
20. Vayssière, J.-L., P.X. Petit, Y. Risler, and B. Mignotte. 1994. Commitment to apoptosis is associated with changes in mitochondrial biogenesis and activity in SV40 conditional cell lines. *Proc. Natl. Acad. Sci. USA.* 91:11752–11756.
21. Newmeyer, D.D., D.M. Farschon, and J.C. Reed. 1994. Cell-free apoptosis in xenopus egg extracts: inhibition by Bcl-2 and requirement for an organelle fraction enriched in mitochondria. *Cell.* 79:353–364.
22. Monaghan, P., D. Robertson, T.A.S. Amos, M.J.S. Dyer, D.Y. Mason, and M.F. Greaves. 1992. Ultrastructural localization of Bcl-2 protein. *J. Histochem. Cytochem.* 40:1819–1825.
23. Nguyen, M., P.E. Branton, P.A. Walton, Z.N. Oltvai, S.J. Korsmeyer, and G.C. Shore. 1994. Role of membrane anchor domain of Bcl-2 in suppression of apoptosis caused by E1B-defective adenovirus. *J. Biol. Chem.* 269:16521–16524.
24. Green, D.R., A. Mahboubi, W. Nishioka, S. Oja, F. Echeverri, Y. Shi, J. Glynn, Y. Yang, J. Ashwell, and R. Bissonnette. 1994. Promotion and inhibition of activation-induced apoptosis in T-cell hybridomas by oncogenes and related signals. *Immunol. Rev.* 142:321–342.
25. Aten, J., P. Prigent, P. Poncet, C. Blanpied, N. Claessen, P. Druet, and F. Hirsch. 1995. Mercuric chloride-induced programmed cell death of a murine T cell hybridoma. I. Effect of the proto-oncogene Bcl-2. *Cell. Immunol.* 161:98–106.
26. Obeid, L.M., C.M. Linardic, L.A. Karolak, and Y.A. Hannun. 1993. Programmed cell death induced by ceramide. *Science (Wash. DC).* 259:1769–1771.
27. Wright, S.C., P. Kumar, A.W. Tam, N. Shen, M. Varma, and J.W. Larrick. 1992. Apoptosis and DNA fragmentation precede TNF-induced cytolysis in U937 cells. *J. Cell. Biochem.* 48:344–355.
28. Cuende, E., J.E. Alés-Martínez, L. Ding, M. González-García, C. Martínez-A., and G. Nuñez. 1993. Programmed cell death by Bcl-2-dependent and -independent mechanisms in B cell lymphoma cells. *EMBO (Eur. Mol. Biol. Organ.) J.* 12:1555–1560.
29. Smiley, S.T. 1991. Intracellular heterogeneity in mitochondrial membrane potential revealed by a J-aggregate-forming lipophilic cation JC-1. *Proc. Natl. Acad. Sci. USA.* 88:3671–3675.
30. Schlegel, R.A., M. Stevens, K. Lumley-Sapansky, and P. Williamson. 1993. Altered lipid packing identifies apoptotic thymocytes. *Immunol. Lett.* 36:283–288.
31. Petit, J.M., A. Maftah, M.H. Ratinaud, and R. Julien. 1992. 10 N-nonylacridine orange interacts with cardiolipin and allows for the quantification of phospholipids in isolated mitochondria. *Eur. J. Biochem.* 209:267–273.
32. Petit, P.X., J.E. O'Connor, D. Grunwald, and S.C. Brown. 1990. Analysis of the membrane potential of rat- and mouse-liver mitochondria by flow cytometry and possible applications. *Eur. J. Biochem.* 194:389–397.
33. Rothe, G., and G. Valet. 1990. Flow cytometric analysis of respiratory burst activity in phagocytes with hydroethidine and 2',7'-dichlorofluorescin. *J. Leukocyte Biol.* 47:440–448.
34. Nicoletti, I., G. Migliorati, M.C. Pagliacci, and C. Riccardi. 1991. A rapid simple method for measuring thymocyte apoptosis by propidium iodide staining and flow cytometry. *J. Immunol. Methods.* 139:271–280.
35. Carter, W.O., P.K. Narayanan, and J.P. Robinson. 1994. Intracellular hydrogen peroxide and superoxide anion detection in endothelial cells. *J. Leukocyte Biol.* 55:253–258.
36. Perandones, C.E., V.A. Illera, D. Peckham, L.L. Stunz, and R.F. Ashman. 1993. Regulation of apoptosis in vitro in mature murine spleen T cells. *J. Immunol.* 151:3521–3529.
37. Baixeras, E., L. Bosca, C. Stauber, A. Gonzalez, A.C. Carrera, J.A. Gonzalo, and C. Martinez-A. 1994. From apoptosis to autoimmunity: insights from the signaling pathways leading to proliferation or to programmed cell death. *Immunol. Rev.* 142:53–91.
38. Cohen, G.M., X.-M. Sun, R.T. Snowden, M.G. Ormerod, and D. Dinsdale. 1993. Identification of a transitional preapoptotic population of thymocytes. *J. Immunol.* 151:566–574.
39. Petronilli, V., C. Cola, S. Massari, R. Colonna, and P. Bernardi. 1993. Physiological effectors modify voltage-sensing by the cyclosporin A-sensitive mitochondrial permeability transition pore. *J. Biol. Chem.* 268:21939–21945.
40. Crompton, M., H. Ellinger, and A. Costi. 1988. Inhibition by cyclosporin A of a Ca^{2+}-dependent pore in heart mitochondria activated by inorganic phosphate and oxidative stress. *Biochem. J.* 255:357–360.
41. Pastorino, J.G., J.W. Snyder, A. Serroni, J.B. Hoek, and J.L. Farber. 1993. Cyclosporin and carnitine prevent the anoxic death of cultured hepatocytes by inhibiting the mitochondrial permeability transition. *J. Biol. Chem.* 268:13791–13798.
42. Bernardi, P. 1992. Modulation of the mitochondrial cyclosporin A-sensitive permeability transition pore by the proton electrochemical gradient. *J. Biol. Chem.* 267:8834–8839.
43. Broekemeier, K.M., R.J. Krebsbach, and D.R. Pfeiffer. 1994. Inhibition of the mitochondrial Ca^{2+} uniporter by pure and impure ruthenium red. *Mol. Cell. Biochem.* 139:33–40.
44. Hennet, T., C. Richter, and E. Peterhans. 1993. Tumour necrosis factor-α induces superoxide anion production in mitochondria of L929 cells. *Biochem. J.* 289:587–592.
45. Nishikawa, M., S. Nojima, T. Akiyama, U. Sankawa, and K. Inoue. 1984. Interaction of digitonin and its analogs with membrane cholesterol. *J. Biochem.* 96:1231–1239.
46. Daum, G. 1985. Lipids of mitochondria. *Biochim. Biophys. Acta.* 822:1–42.
47. Behl, C., J.B. Davis, R. Lesley, and D. Schubert. 1994. Hydrogen peroxide mediates amyloid β protein toxicity. *Cell.* 77: 817–827.
48. Konstantinov, A.A., A.V. Peskin, E.Y. Popova, G.B. Khomutov, and E. Ruuge. 1987. Superoxide generation by the respiratory chain of tumor mitochondria. *Biochim. Biophys. Acta.* 894:1–10.
49. Schlame, M., S. Brody, and K.Y. Hostetler. 1993. Mitochondrial cardiolipin in diverse eukaryotes. Comparison of biosynthetic reactions and molecular acyl species. *Eur. J. Biochem.* 212:727–735.
50. Maftah, A., J.-M. Petit, M.-H. Ratinaud, and R. Julien. 1989. 10-N Nonyl-acridine orange: a fluorescent probe which stains mitochondria independently of their energetic state. *Biochem. Biophys. Res. Commun.* 164:185–190.
51. Lyons, A.B., K. Samuel, A. Sanderson, and A.H. Maddy. 1992. Simultaneous analysis of immunophenotype and apoptosis of murine thymocytes by single laser flow cytometry. *Cytometry.* 13:809–821.

52. Mower, D.A., D.W. Peckham, V.A. Illera, J.K. Fishbaugh, L.L. Stunz, and R.F. Ashman. 1994. Decreased membrane phospholipid packing and decreased cell size precede DNA cleavage in mature mouse B cell apoptosis. *J. Immunol.* 152:4832–4842.
53. Fadok, V.A., D.R. Voelker, P.A. Campbell, J.J. Cohen, D.L. Bratton, and P.M. Henson. 1992. Exposure of phophatidylserine on the surface of apoptotic lymphocytes triggers specific recognition and removal by macrophages. *J. Immunol.* 148: 2207–2216.
54. Haimovitz-Friedman, A., C.-C. Kan, D. Ehleitner, R.S. Persaud, M. McLoughlin, Z. Fuks, and R.N. Kolesnick. 1994. Ionizing radiation acts on cellular membranes to generate ceramide and initiate apoptosis. *J. Exp. Med.* 180:525–535.
55. Smets, L.A., J. Van den Berg, D. Acton, B. Top, H. van Rooij, and M. Verwijs-Janssen. 1994. BCL-2 expression and mitochondrial activity in leukemic cells with different sensitivity to glucocorticoid-induced apoptosis. *Blood.* 5:1613–1619.
56. Wolvetang, E.J., K.L. Johnson, K. Krauer, S.J. Ralph, and A.W. Linnane. 1994. Mitochondrial respiratory chain inhibitors induce apoptosis. *FEBS Lett.* 339:40–44.
57. Hartley, A., J.M. Stone, C. Heron, J.M. Cooper, and A.H.V. Schapira. 1994. Complex I inhibitors induce dose-dependent apoptosis in PC12 cells: relevance to Parkinson disease. *J. Neurochem.* 63:1987–1990.
58. Van den Bogert, C., B. Dontje, T. Melis, C. Van der Veen, and A. Kroon. 1988. Inhibition of mitochondrial protein synthesis influences the glucocorticoid sensitivity of lymphoid cells. *Biochim. Biophys. Acta.* 972:302–309.
59. Attardi, G., and G. Schatz. 1988. Biogenesis of mitochondria. *Annu. Rev. Cell Biol.* 4:289–333.
60. Nordeen, S.K., and D.A. Young. 1976. Glucocorticoid action on rat thymic lymphocytes. *J. Biol. Chem.* 251:7295–7303.
61. Osborne, B.A., S.W. Smith, Z.-G. Liu, K.A. McLaughlin, L. Grimm, and L.M. Schwartz. 1994. Identification of genes induced during apoptosis in T cells. *Immunol. Rev.* 142:301–320.
62. Jacobson, M.D., J.F. Burne, M.P. King, T. Miyashita, J.C. Reed, and M.C. Raff. 1993. Bcl-2 blocks apoptosis in cells lacking mitochondrial DNA. *Nature (Lond.).* 361:365–369.
63. Skowronek, P., O. Haferkamp, and G. Rödel. 1992. A fluorescence-microscopic and flow-cytometric study of HELA cells with an experimentally induced respiratory deficiency. *Biochem. Biophys. Res. Commun.* 187:991–998.
64. Schulze-Osthoff, K., R. Beyaert, V. Vandevoorde, G. Haegeman, and W. Fiers. 1993. Depletion of the mitochondrial electron transport abrogates the cytotoxic and gene-inductive effects of TNF. *EMBO (Eur. Mol. Biol. Organ.) J.* 12:3095–3104.
65. Schulze-Osthoff, K., P.H. Krammer, and W. Dröge. 1994. Divergent signalling via APO-1/Fas and the TNF receptor, two homologous molecules involved in physiological cell death. *EMBO (Eur. Mol. Biol. Organ.) J.* 13:4587–4596.
66. Zoratti, M., and I. Szabò. 1995. The mitochondrial permeability transition. *Biochim. Biophys. Acta.* In press.
67. Petronilli, V., A. Nicolli, P. Costantini, R. Colonna, and P. Bernardi. 1994. Regulation of the permeability transition pore, a voltage-dependent mitochondrial channel inhibited by cyclosporin A. *Biochim. Biophys. Acta.* 1187:255–259.
68. Zacharchuk, C.M., M. Mercep, and J.D. Ashwell. 1991. Thymocyte activation and death: a mechanism for molding the T cell repertoire. *Ann. NY Acad. Sci.* 636:52–70.
69. Zhang, Y., O. Marcillat, C. Giulivi, L. Ernster, and K.J.A. Davies. 1990. The oxidative inactivation of mitochondrial electron transport chain components and ATPase. *J. Biol. Chem.* 265:16330–16336.
70. Bernardi, P., S. Vassanelli, P. Veronese, R. Colonna, I. Szabo, and M. Zoratti. 1992. Modulation of the mitochondrial permeability transition pore. Effect of protons and divalent cations. *J. Biol. Chem.* 267:2934–2939.
71. Kan, O., S.A. Baldwin, and A.D. Whetton. 1994. Apoptosis is regulated by the rate of glucose transport in an interleukin 3–dependent cell line. *J. Exp. Med.* 180:917–923.